

The Phases of QCD in Heavy Ion Collisions and Compact Stars

Krishna Rajagopal¹

*Center for Theoretical Physics, Massachusetts Institute of Technology
Cambridge, MA 02139*

Abstract. I review arguments for the existence of a critical point E in the QCD phase diagram as a function of temperature T and baryon chemical potential μ . I describe how heavy ion collision experiments at the SPS and RHIC can discover the tell-tale signatures of such a critical point, thus mapping this region of the QCD phase diagram. I then review the phenomena expected in cold dense quark matter: color superconductivity and color-flavor locking. I close with a snapshot of ongoing explorations of the implications of recent developments in our understanding of cold dense quark matter for the physics of compact stars.

The QCD vacuum in which we live, which has the familiar hadrons as its excitations, is but one phase of QCD, and far from the simplest one at that. One way to better understand this phase and the nonperturbative dynamics of QCD more generally is to study other phases and the transitions between phases. We are engaged in a voyage of exploration, mapping the QCD phase diagram as a function of temperature T and baryon number chemical potential μ . Because QCD is asymptotically free, its high temperature and high baryon density phases are more simply and more appropriately described in terms of quarks and gluons as

¹⁾ One version of this review is to appear in the Comments on Nuclear and Particle Physics section of Comments on Modern Physics. Other versions were contributed to the Proceedings of the Conference on Intersections of Nuclear and Particle Physics, Québec, May 2000 and to the Proceedings of the 40th Zakopane School of Theoretical Physics, June 2000. Many thanks to the CIPANP organizers for a conference which was stimulating precisely because it addressed so many facets of the intersection between nuclear and particle physics. Many thanks to the Zakopane organizers for a school which brought condensed matter physics and physicists and particle physics and physicists together, and for an excuse to visit a beautiful part of the world for the first time. I am grateful to M. Alford, B. Berdnikov, J. Berges, J. Bowers, E. Shuster, E. Shuryak, M. Stephanov and F. Wilczek for fruitful collaboration. I acknowledge helpful discussions with P. Bedaque, D. Blaschke, I. Bombaci, G. Carter, D. Chakrabarty, J. Madsen, C. Nayak, M. Prakash, D. Psaltis, S. Reddy, M. Ruderman, T. Schäfer, A. Sedrakian, D. Son, I. Wasserman and F. Weber. This work is supported in part by the U.S. Department of Energy (D.O.E.) under cooperative research agreement #DF-FC02-94ER40818 and by a DOE OJI Award and by the Alfred P. Sloan Foundation. Preprint MIT-CTP-3020.

degrees of freedom, rather than hadrons. The chiral symmetry breaking condensate which characterizes the vacuum phase melts away. At high temperatures, in the resulting quark-gluon plasma (QGP) phase all of the symmetries of the QCD Lagrangian are unbroken and the excitations have the quantum numbers of quarks and gluons. At high densities, on the other hand, quarks form Cooper pairs and new condensates develop. The formation of such superconducting phases [1–5] requires only weak attractive interactions; these phases may nevertheless break chiral symmetry [5] and have excitations with the same quantum numbers as those in a confined phase [5–8]. These cold dense quark matter phases may arise in the core of neutron stars; mapping this region of the phase diagram requires an interplay between theory and neutron star phenomenology. We describe efforts in this direction in Section IV. A central goal of the experimental heavy ion physics program is to explore and map the higher temperature regions of the QCD phase diagram. Recent theoretical developments suggest that a key qualitative feature, namely a critical point which in a sense defines the landscape to be mapped, may be within reach of discovery and analysis as data is taken at several different energies [9,10]. The discovery of the critical point would transform this region of the map of the QCD phase diagram from one based only on reasonable inference from universality, lattice gauge theory and models into one with a solid experimental basis.

I THE CRITICAL POINT

We begin our walk through the phase diagram at zero baryon number density, with a brief review [11] of the phase changes which occur as a function of temperature. That is, we begin by restricting ourselves to the vertical axis in Figures 1 through 4. This slice of the phase diagram was explored by the early universe during the first tens of microseconds after the big bang and can be studied in lattice simulations. As heavy ion collisions are performed at higher and higher energies, they create plasmas with a lower and lower baryon number to entropy ratio and therefore explore regions of the phase diagram closer and closer to the vertical axis.

In QCD with two massless quarks ($m_{u,d} = 0$; $m_s = \infty$; Figure 1) the vacuum phase, with hadrons as excitations, is characterized by a chiral condensate $\langle \bar{\psi}_{L\alpha a} \psi_R^{\alpha a} \rangle$. (The color index α is summed over the three colors; the flavor index a is summed over the two flavors.) Whereas the QCD Lagrangian is invariant under separate global flavor rotations of the left-handed and right-handed quarks, the presence of the chiral condensate spontaneously breaks $SU(2)_L \times SU(2)_R$ to the subgroup $SU(2)_{L+R}$, in which only simultaneous flavor rotations of L and R quarks are allowed. In this way, locking left- and right-handed rotations breaks global symmetries and results in three massless Goldstone bosons, the pions. The chiral order parameter, a 2×2 matrix M^{ab} in flavor space, can be written in terms of four real fields σ and $\vec{\pi}$ as

$$\langle \bar{\psi}_{L\alpha}^a \psi_R^{\alpha b} \rangle = M^{ab} = \sigma \delta^{ab} + \vec{\pi} \cdot (\vec{\tau})^{ab} , \quad (1)$$

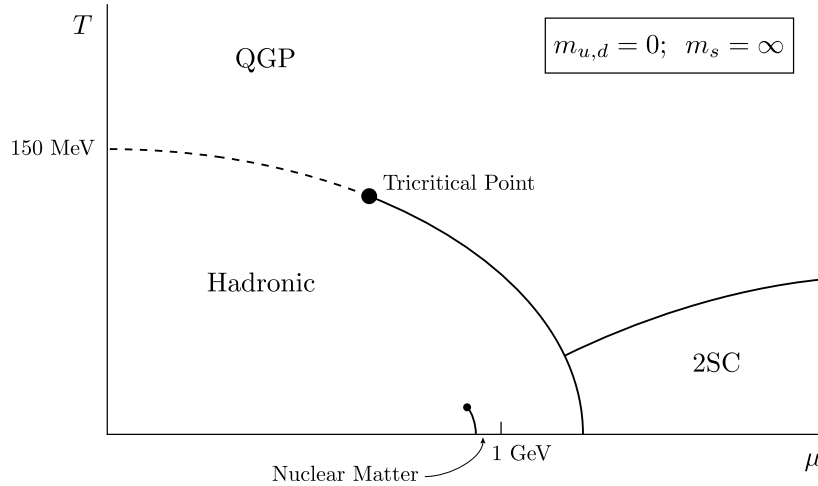


FIGURE 1. QCD Phase diagram for two massless quarks. Chiral symmetry is broken in the hadronic phase and is restored elsewhere in the diagram. The chiral phase transition changes from second to first order at a tricritical point. The phase at high density and low temperature is a color superconductor in which up and down quarks with two out of three colors pair and form a condensate. The transition between this 2SC phase and the QGP phase is likely first order. The transition on the horizontal axis between the hadronic and 2SC phases is first order. The transition between a nuclear matter “liquid” and a gas of individual nucleons is also marked; it ends at a critical point at a temperature of order 10 MeV, characteristic of the forces which bind nucleons into nuclei.

where the $\vec{\tau}$ are the three Pauli matrices. $SU(2)_L$ and $SU(2)_R$ rotations act on M^{ab} from the left and right, respectively. The order parameter can also be written as a four component scalar field $\phi = (\sigma, \vec{\pi})$ and the $SU(2)_L \times SU(2)_R$ rotations are then simply $O(4)$ rotations of ϕ . In this language, the symmetry breaking pattern $SU(2)_L \times SU(2)_R \rightarrow SU(2)_{L+R}$ is described as $O(4) \rightarrow O(3)$: in the vacuum, $\langle \phi \rangle \neq 0$ and this condensate picks a direction in $O(4)$ -space. The direction in which the condensate points is conventionally taken to be the σ direction. In the presence of $\langle \sigma \rangle \neq 0$, the $\vec{\pi}$ excitations are excitations of the direction in which $\langle \phi \rangle$ is pointing, and are therefore massless goldstone modes.

At nonzero but low temperature, one finds a gas of pions, the analogue of a gas of spin-waves, but $\langle \phi \rangle$ is still nonzero. Above some temperature T_c , entropy wins over order (the direction in which ϕ points is scrambled) and $\langle \phi \rangle = 0$. The phase transition at which chiral symmetry is restored is likely second order and belongs to the universality class of $O(4)$ spin models in three dimensions [12]. Below T_c , chiral symmetry is broken and there are three massless pions. At $T = T_c$, there are four massless degrees of freedom: the pions and the sigma. Above $T = T_c$, the pion and sigma correlation lengths are degenerate and finite.

In nature, the light quarks are not massless. Because of this explicit chiral symmetry breaking, the second order phase transition is replaced by an analytical crossover: physics changes dramatically but smoothly in the crossover region, and

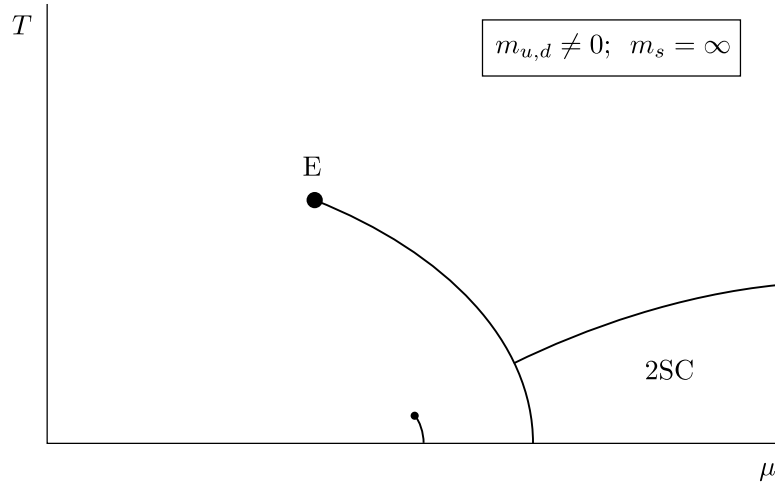


FIGURE 2. QCD phase diagram for two light quarks. Qualitatively as in Figure 1, except that the introduction of light quark masses turns the second order phase transition into a smooth crossover. The tricritical point becomes the critical endpoint E , which can be found in heavy ion collision experiments.

no correlation length diverges. Thus, in Figure 2, there is no sharp boundary on the vertical axis separating the low temperature hadronic world from the high temperature quark-gluon plasma. This picture is consistent with present lattice simulations [13,14], which suggest $T_c \sim 140 - 190$ MeV [15,14].

Arguments based on a variety of models [16,17,3,4,18,19] indicate that the chiral symmetry restoration transition is first order at large μ . (In Section III, we describe the color superconducting (2SC) phase of cold dense quark matter which occurs at values of μ above this first order transition; the fact that this is a transition in which two different condensates compete strengthens the argument that this transition is first order [18,20].) This suggests that the phase diagram features a critical point E at which the line of first order phase transitions present for $\mu > \mu_E$ ends, as shown in Figure 2.² At μ_E , the phase transition is second order and is in the Ising universality class [18,19]. Although the pions remain massive, the correlation length in the σ channel diverges due to universal long wavelength fluctuations of the order parameter. This results in characteristic signatures, analogues of critical opalescence in the sense that they are unique to collisions which freeze out near the critical point, which can be used to discover E [9,10].

Returning to the $\mu = 0$ axis, universal arguments [12], again backed by lattice simulation [13], tell us that if the strange quark were as light as the up and down quarks, the transition would be first order, rather than a smooth crossover. This means that if one could dial the strange quark mass m_s , one would find a critical m_s^c at which the transition as a function of temperature is second order [22,11].

²⁾ If the up and down quarks were massless, E would be a tricritical point [21], at which the first order transition becomes second order. See Figure 1.

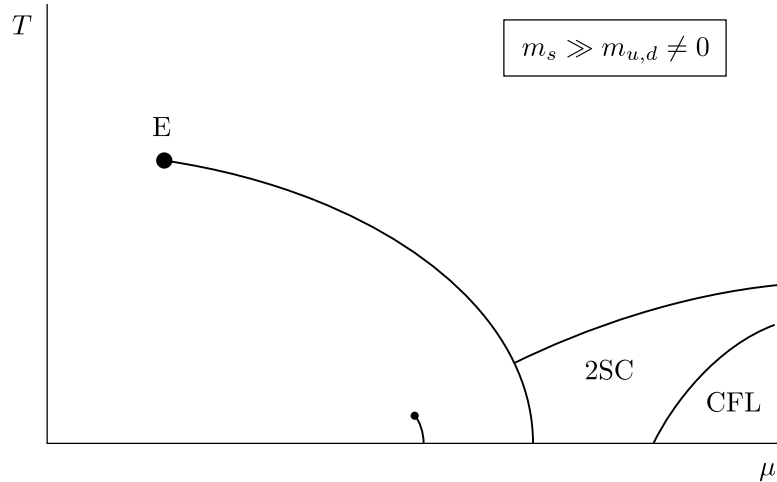


FIGURE 3. QCD phase diagram for two light quarks and a strange quark with a mass comparable to that in nature. The presence of the strange quark shifts E to the left, as can be seen by comparing with Figure 2. At sufficiently high density, cold quark matter is necessarily in the CFL phase in which quarks of all three colors and all three flavors form Cooper pairs. The diquark condensate in the CFL phase breaks chiral symmetry, and this phase has the same symmetries as baryonic matter which is dense enough that the nucleon and hyperon densities are comparable. The phase transition between the CFL and 2SC phases is first order.

Figures 2, 3 and 4 are drawn for a sequence of decreasing strange quark masses. Somewhere between Figures 3 and 4, m_s is decreased below m_s^c and the transition on the vertical axis becomes first order. The value of m_s^c is an open question, but lattice simulations suggest that it is about half the physical strange quark mass [23,24]. These results are not yet conclusive [25] but if they are correct then the phase diagram in nature is as shown in Figure 3, and the phase transition at low μ is a smooth crossover.

These observations fit together in a simple and elegant fashion. If we could vary m_s , we would find that as m_s is reduced from infinity to m_s^c , the critical point E in the (T, μ) plane moves toward the $\mu = 0$ axis [9]. This is shown in Figures 2-4. In nature, E is at some nonzero T_E and μ_E . When m_s is reduced to m_s^c , between Figure 3 and Figure 4, μ_E reaches zero. Of course, experimentalists cannot vary m_s . They can, however, vary μ . AGS collisions with center of mass energy $\sqrt{s} = 5$ AGeV create fireballs which freeze out near $\mu \sim 500 - 600$ MeV [26]. SPS collisions with $\sqrt{s} = 17$ AGeV create fireballs which freeze out near $\mu \sim 200 - 300$ MeV [26]. In time, we will also have data from SPS collisions with $\sqrt{s} = 9$ AGeV and from RHIC collisions with $\sqrt{s} = 56, 130$ and 200 AGeV and other energies.³ By dialing \sqrt{s} and thus μ , experimenters can find the critical point E .

³⁾ The first data from RHIC collisions at $\sqrt{s} = 56$ AGeV and $\sqrt{s} = 130$ AGeV have already appeared [27]. This bodes well for the analyses to come.

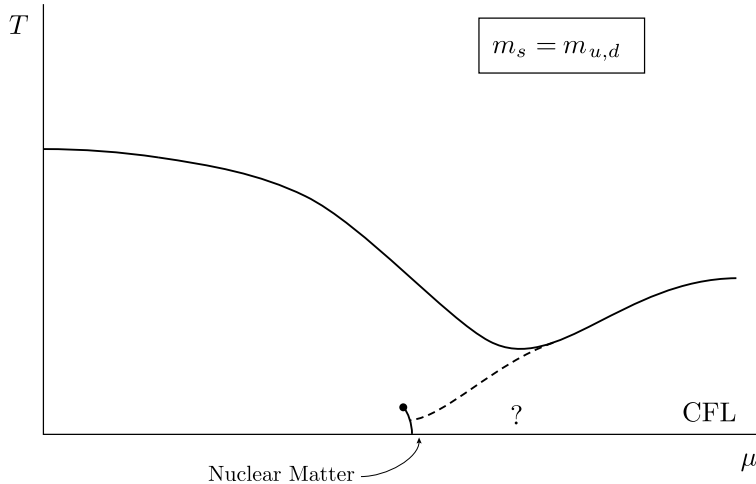


FIGURE 4. QCD phase diagram for three quarks which are degenerate in mass and which are either massless or light. The CFL phase and the baryonic phase have the same symmetries and may be continuously connected. The dashed line denotes the critical temperature at which baryon-baryon (or quark-quark) pairing vanishes; the region below the dashed line is superfluid. Chiral symmetry is broken everywhere below the solid line, which is a first order phase transition. The question mark serves to remind us that although no transition is required in this region, transition(s) may nevertheless arise as the magnitude of the gap increases qualitatively in going from the hypernuclear to the CFL phase. For quark masses as in nature, the high density region of the map may be as shown in Figure 3 or may be closer to that shown here, albeit with transition(s) in the vicinity of the question mark associated with the onset of nonzero hyperon density and the breaking of $U(1)_S$ [7].

II DISCOVERING THE CRITICAL POINT

We hope that the study of heavy ion collisions will, in the end, lead both to a quantitative study of the properties of the quark-gluon plasma phase at temperatures well above the transition and to a quantitative understanding of how to draw the phase transition region of the phase diagram. Probing the partonic matter created early in the collision relies on a suite of signatures including: the use of J/Ψ mesons, charmed mesons, and perhaps the Υ as probes; the energy loss of high momentum partons and consequent effects on the high- p_T hadron spectrum; and the detection of photons and dileptons over and above those emitted in the later hadronic stages of the collision. I will not review this program here. Instead, I focus on signatures of the critical point. The map of the QCD phase diagram which I have sketched so far is simple, coherent and consistent with all we know theoretically; the discovery of the critical point would provide an experimental foundation for the central qualitative feature of the landscape. This discovery would in addition confirm that in higher energy heavy ion collisions and in the big bang, the QCD phase transition is a smooth crossover. Furthermore, the discovery of collisions which create matter that freezes out near E would imply that conditions above

the transition existed prior to freezeout, and would thus make it much easier to interpret the results of other experiments which study those observables which can probe the partonic matter created early in the collision.

We theorists must clearly do as much as we can to tell experimentalists *where* and *how* to find E . The “where” question, namely the question of predicting the value of μ_E and thus suggesting the \sqrt{s} to use to find E , is much harder for us to answer. First, as we stress further in the next Section, *ab initio* analysis of QCD in its full glory — i.e. lattice calculations — are at present impossible at nonzero μ . We must therefore rely on models. Second, an intrinsic feature of the picture we have described is that μ_E is sensitive to the mass of the strange quark, and therefore particularly hard to predict. Crude models suggest that μ_E could be $\sim 600 - 800$ MeV in the absence of the strange quark [18,19]; this in turn suggests that in nature μ_E may have of order half this value, and may therefore be accessible at the SPS if the SPS runs with $\sqrt{s} < 17$ AGeV. However, at present theorists cannot predict the value of μ_E even to within a factor of two. The SPS can search a significant fraction of the parameter space; if it does not find E , it will then be up to the RHIC experiments to map the $\mu < 200$ MeV region.

Although we are trying to be helpful with the “where” question, we are not very good at answering it quantitatively. This question can only be answered convincingly by an experimental discovery. What we theorists *can* do reasonably well is to answer the “how” question, thus enabling experimenters to answer “where”. This is the goal of a recent paper by Stephanov, myself and Shuryak [10]. The signatures we have proposed are based on the fact that E is a genuine thermodynamic singularity at which susceptibilities diverge and the order parameter fluctuates on long wavelengths. The resulting signatures are *nonmonotonic* as a function of \sqrt{s} : as this control parameter is varied, we should see the signatures strengthen and then weaken again as the critical point is approached and then passed.

The critical point E can also be sought by varying control parameters other than \sqrt{s} . Ion size, centrality selection and rapidity selection can all be varied. The advantage of using \sqrt{s} is that we already know (by comparing results from the AGS and SPS) that dialing it changes the freeze out chemical potential μ , which is the goal in a search for E .

The simplest observables we analyze are the event-by-event fluctuations of the mean transverse momentum of the charged particles in an event, p_T , and of the total charged multiplicity in an event, N . We calculate the magnitude of the effects of critical fluctuations on these and other observables, making predictions which, we hope, will allow experiments to find E . As a necessary prelude, we analyze the contribution of noncritical thermodynamic fluctuations. We compare the noncritical fluctuations of an equilibrated resonance gas to the fluctuations measured by NA49 at $\sqrt{s} = 17$ AGeV [28]. The observed fluctuations are as perfect Gaussians as the data statistics allow, as expected for freeze-out from a system in thermal equilibrium. The data on multiplicity fluctuations show evidence for a nonthermodynamic contribution, which is to be expected since the extensive quantity N is sensitive to the initial size of the system and thus to nonthermodynamic effects like

variation in impact parameter. The contribution of such effects to the fluctuations have now been estimated [29,30]; the combined thermodynamic and nonthermodynamic fluctuations are in satisfactory agreement with the data [30]. The width of the event-by-event distribution⁴ of mean p_T is in good agreement with predictions based on noncritical thermodynamic fluctuations. That is, NA49 data are consistent with the hypothesis that almost all the observed event-by-event fluctuation in mean p_T , an intensive quantity, is thermodynamic in origin. This bodes well for the detectability of systematic changes in thermodynamic fluctuations near E .

One analysis described in detail in Ref. [10] is based on the ratio of the width of the true event-by-event distribution of the mean p_T to the width of the distribution in a sample of mixed events. This ratio was called \sqrt{F} . NA49 has measured $\sqrt{F} = 1.002 \pm 0.002$ [28,10], which is consistent with expectations for noncritical thermodynamic fluctuations.⁵ Critical fluctuations of the σ field, i.e. the characteristic long wavelength fluctuations of the order parameter near E , influence pion momenta via the (large) $\sigma\pi\pi$ coupling and increase \sqrt{F} [10]. The effect is proportional to $\xi_{\text{freezeout}}^2$, where $\xi_{\text{freezeout}}$ is the σ -field correlation length of the long-wavelength fluctuations at freezeout [10]. If $\xi_{\text{freezeout}} \sim 3$ fm (a reasonable estimate, as we describe below) the ratio \sqrt{F} increases by $\sim 3 - 5\%$, ten to twenty times the statistical error in the present measurement [10]. This observable is valuable because data on it has been analyzed and presented by NA49, and it can therefore be used to learn that Pb+Pb collisions at 158 AGeV do *not* freeze out near E . The $3 - 5\%$ nonmonotonic variation in \sqrt{F} as a function of \sqrt{s} which we predict is easily detectable but is not so large as to make one confident of using this alone as a signature of E .

Once E is located, however, other observables which are more sensitive to critical effects will be more useful. For example, a $\sqrt{F_{\text{soft}}}$, defined using only the softest 10% of the pions in each event, will be much more sensitive to the critical long wavelength fluctuations. The higher p_T pions are less affected by the σ fluctuations [10], and these relatively unaffected pions dominate the mean p_T of all the pions in the event. This is why the increase in \sqrt{F} near the critical point will be much less than that of $\sqrt{F_{\text{soft}}}$. Depending on the details of the cuts used to define it, $\sqrt{F_{\text{soft}}}$ should be enhanced by many tens of percent in collisions passing near E . Ref. [10] suggests other such observables, and more can surely be found.

The multiplicity of soft pions is an example of an observable which may be

⁴) This width can be measured even if one observes only two pions per event [31]; large acceptance data as from NA49 is required in order to learn that the distribution is Gaussian, that thermodynamic predictions may be valid, and that the width is therefore the only interesting quantity to measure.

⁵) In an infinite system made of classical particles which is in thermal equilibrium, $\sqrt{F} = 1$. Bose effects increase \sqrt{F} by $1 - 2\%$ [32,10]; an anticorrelation introduced by energy conservation in a finite system — when one mode fluctuates up it is more likely for other modes to fluctuate down — decreases \sqrt{F} by $1 - 2\%$ [10]; two-track resolution also decreases \sqrt{F} by $1 - 2\%$ [28]. The contributions due to correlations introduced by resonance decays and due to fluctuations in the flow velocity are each much smaller than 1% [10].

used to detect the critical fluctuations without an event-by-event analysis. The post-freezeout decay of sigma mesons, which are copious and light at freezeout near E and which decay subsequently when their mass increases above twice the pion mass, should result in a population of pions with $p_T \sim m_\pi/2$ which appears only for freezeout near the critical point [10]. If $\xi_{\text{freezeout}} > 1/m_\pi$, this population of unusually low momentum pions will be comparable in number to that of the “direct” pions (i.e. those which were pions at freezeout) and will result in a large signature. This signature is therefore certainly large for $\xi_{\text{freezeout}} \sim 3$ fm and would not increase much further if $\xi_{\text{freezeout}}$ were larger still.

The variety of observables which should *all* vary nonmonotonically with \sqrt{s} (and should all peak at the same \sqrt{s}) is sufficiently great that if it were to turn out that $\mu_E < 200$ MeV, making E inaccessible to the SPS, all four RHIC experiments could play a role in the study of the critical point.

The purpose of Ref. [33] is to estimate how large $\xi_{\text{freezeout}}$ can become, thus making the predictions of Ref. [10] for the magnitude of various signatures more quantitative. The nonequilibrium dynamics analyzed in Ref. [33] is guaranteed to occur in a heavy ion collision which passes near E , even if local thermal equilibrium is achieved at a higher temperature during the earlier evolution of the plasma created in the collision. If this plasma were to cool arbitrarily slowly, ξ would diverge at T_E . However, it would take an infinite time for ξ to grow infinitely large. Indeed, near a critical point, the longer the correlation length, the longer the equilibration time, and the slower the correlation length can grow. This critical slowing down means that the correlation length cannot grow sufficiently fast for the system to stay in equilibrium. We use the theory of dynamical critical phenomena to describe the effects of critical slowing down of the long wavelength dynamics near E on the time development of the correlation length. The correlation length does not have time to grow as large as it would in equilibrium: we find $\xi_{\text{freezeout}} \sim 2/T_E \sim 3$ fm for trajectories passing near E . Although critical slowing down hinders the growth of ξ , it also slows the decrease of ξ as the system continues to cool below the critical point. As a result, ξ does not decrease significantly between the phase transition and freezeout.

Our results depend on the universal function describing the equilibrium behavior of ξ near the Ising critical point E , on the universal dynamical exponent z describing critical slowing down (perturbations away from equilibrium relax toward equilibrium on a timescale which scales with ξ like $A\xi^z$ [34]), on the nonuniversal constant A , the nonuniversal constants which relate $(T - T_E)$ and $(\mu - \mu_E)$ to dimensionless Ising model variables, on T_E which we take to be ~ 140 MeV, and finally on the cooling rate $|dT/dt|$ which we estimate to be 4 MeV/fm [35,33].

Our estimate that ξ does not grow larger than $2/T_E$ is robust in three senses. First, it depends very little on the angle with which the trajectory passes through E . Second, it turns out to depend on only one combination of all the nonuniversal quantities which play a role. We call this parameter a ; it is proportional to $|dT/dt|^{-1}$. Third, our results do not depend sensitively on a . We show that the

maximum value of ξ scales like $a^{\frac{\nu/\beta\delta}{1+z\nu/\beta\delta}} \approx a^{0.215}$ [33].⁶ Thus, for example, $|dT/dt|$ would have to be a factor of 25 smaller than we estimate in order for ξ to grow to $4/T_E$ instead of $2/T_E$. Although our results are robust in this sense, they cannot be treated as precise because our assumption that the dynamics of ξ in QCD is described by the universal classical dynamics of the three-dimensional Ising model only becomes precise if $\xi \gg 1/T_E$, while our central result is that ξ does not grow beyond $\sim 2/T_E$. A 3 + 1-dimensional quantum field theoretical treatment of the interplay between cooling and the dynamics of critical slowing down is not yet available, but promising first steps in this direction can be found in Ref. [40].

A result which is of great importance in the planning of experimental searches is that one need not hit E precisely in order to find it. Our analysis demonstrates that if one were to do a scan with collisions at many finely spaced values of the energy and thus μ , one would see signatures of E with approximately the same magnitude over a broad range of μ . The magnitude of the signatures will not be narrowly peaked as μ is varied. As long as one gets close enough to E that the equilibrium correlation length is $(2 - 3)/T_E$, the actual correlation length ξ will grow to $\sim 2/T_E$. There is no advantage to getting closer to E , because critical slowing down prevents ξ from getting much larger even if ξ_{eq} does. Data at many finely spaced values of μ is *not* called for.

As described above, knowing that we are looking for $\xi_{freezeout} \sim 3$ fm allows us [33] to make quantitative estimates of the magnitude of the signatures of E described in detail in Ref. [10]. Together, the excess multiplicity at low momentum (due to post-freezeout sigma decays) and the excess event-by-event fluctuation of the momenta of the low momentum pions (due to their coupling to the order parameter which is fluctuating with correlation length $\xi_{freezeout}$) should allow a convincing detection of the critical point E . Both should behave nonmonotonically as the collision energy, and hence μ , are varied. Both should peak for those heavy ion collisions which freeze out near E , with $\xi_{freezeout} \sim 3$ fm.

We have learned much from the beautiful gaussian event-by-event fluctuations observed by NA49. The magnitude of these fluctuations are consistent with the hypothesis that the hadronic system at freezeout is in approximate thermal equilibrium. These and other data show none of the non-gaussian features that would signal that the system had been driven far from equilibrium either by a rapid traversal of the transition region or by the bubbling that would occur near a strong first order phase transition. There is also no sign of the enhanced, but still gaussian, fluctuations which would signal freezeout near the critical point E . Combining these observations with the observation of tantalizing indications that the matter created in SPS collisions is not well described at early times by hadronic models [41]

⁶) A scaling law of this form (of course with different numerical values for the exponents) relating the maximum correlation length which is reached to the cooling rate was first discovered in the theory of defect formation at a second order phase transition [36]. It has been tested in this context in numerical simulations [37] and, furthermore, is supported by data from experiments on liquid crystals [38] and superfluid ^3He [39].

suggests that collisions at the SPS may be exploring the crossover region to the left of the critical point E , in which the matter is not well-described as a hadron gas but is also not well-described as a quark-gluon plasma. This speculation could be confirmed in two ways. First, if the SPS is probing the crossover region then the coming experiments at RHIC may discover direct signatures of an early partonic phase, which are well-described by theoretical calculations beginning from an equilibrated quark-gluon plasma. Second, if $\sqrt{s} = 17$ AGeV collisions are probing the crossover region not far to the left of the critical point E , then SPS data taken at lower energies would result in the discovery of E . If, instead, RHIC were to discover E with $\mu_E < 200$ MeV, that would indicate that the SPS experiments have probed the weakly first order region just to the right of E . Regardless, discovering E would take all the speculation out of mapping this part of the QCD phase diagram.

III COLOR SUPERCONDUCTIVITY AND COLOR-FLAVOR LOCKING

I turn now to recent developments in our understanding of the low temperature, high density regions of the QCD phase diagram. First, a notational confession. It is conventional in the literature on cold dense quark matter to define μ as the *quark* number chemical potential, 1/3 the baryon number chemical potential used in Sections I and II. We make this change from here on. For example, neutron star cores likely have $\mu \sim 400 - 500$ MeV, corresponding to baryon number chemical potentials $\sim 1.2 - 1.5$ GeV in Figures 1-4.

The relevant degrees of freedom in cold dense quark matter are those which involve quarks with momenta near the Fermi surface. At high density, when the Fermi momentum is large, the QCD gauge coupling $g(\mu)$ is small. However, because of the infinite degeneracy among pairs of quarks with equal and opposite momenta at the Fermi surface, even an arbitrarily weak attraction between quarks renders the Fermi surface unstable to the formation of a condensate of quark Cooper pairs. Creating a pair costs no free energy at the Fermi surface and the attractive interaction results in a free energy benefit. Pairs of quarks cannot be color singlets, and in QCD with two flavors of massless quarks the Cooper pairs form in the (attractive) color $\mathbf{\bar{3}}$ channel [1-4]. The resulting condensate creates a gap Δ at the Fermi surfaces of quarks with two out of the three colors and breaks $SU(3)_{\text{color}}$ to an $SU(2)_{\text{color}}$ subgroup, giving mass to five of the gluons by the Anderson-Higgs mechanism. In QCD with two flavors, the Cooper pairs are $ud - du$ flavor singlets and the global flavor symmetry $SU(2)_L \times SU(2)_R$ is intact. There is also an unbroken global symmetry which plays the role of $U(1)_B$. Thus, no global symmetries are broken in this 2SC phase. There must therefore be a phase transition between the 2SC and hadronic phases on the horizontal axis in Figure 1, at which chiral symmetry is restored. This phase transition is first order [3,18,42,20] since it involves a competition between chiral condensation and diquark condensation [18,20]. There need be no transition between the 2SC and quark-gluon plasma phases in

Figure 1 because neither phase breaks any global symmetries. However, this transition, which is second order in mean field theory, is likely first order in QCD due to gauge field fluctuations [18], at least at high enough density [43].

In QCD with three flavors of massless quarks, the Cooper pairs *cannot* be flavor singlets, and both color and flavor symmetries are necessarily broken. The symmetries of the phase which results have been analyzed in [5,6]. The attractive channel favored by one-gluon exchange exhibits “color-flavor locking.” A condensate of the form

$$\langle \psi_L^{\alpha a} \psi_L^{\beta b} \rangle \propto \Delta \epsilon^{\alpha\beta A} \epsilon^{abA} \quad (2)$$

involving left-handed quarks alone, with α, β color indices and a, b flavor indices, locks $SU(3)_L$ flavor rotations to $SU(3)_{\text{color}}$: the condensate is not symmetric under either alone, but is symmetric under the simultaneous $SU(3)_{L+\text{color}}$ rotations.⁷ A condensate involving right-handed quarks alone locks $SU(3)_R$ flavor rotations to $SU(3)_{\text{color}}$. Because color is vectorial, the combined effect of the LL and RR condensates is to lock $SU(3)_L$ to $SU(3)_R$, breaking chiral symmetry.⁸ Thus, in quark matter with three massless quarks, the $SU(3)_{\text{color}} \times SU(3)_L \times SU(3)_R \times U(1)_B$ symmetry is broken down to the global diagonal $SU(3)_{\text{color}+L+R}$ group. A gauged $U(1)$ subgroup of the original symmetry group — a linear combination of one color generator and electromagnetism, which lives within $SU(3)_L \times SU(3)_R$ — also remains unbroken. All nine quarks have a gap. All eight gluons get a mass. There are nine massless Nambu-Goldstone bosons. All the quarks, all the massive vector bosons, and all the Nambu-Goldstone bosons have integer charges under the unbroken gauged $U(1)$ symmetry, which therefore plays the role of electromagnetism. The CFL phase therefore has the same symmetries as baryonic matter with a condensate of Cooper pairs of baryons [6]. Furthermore, many non-universal features of these two phases correspond [6]. This raises the possibility that quark matter and baryonic matter may be continuously connected [6], as shown in Figure 4.

The physics of the CFL phase has been the focus of much recent work [5–8,44–59]. Nature chooses two light quarks and one middle-weight strange quark, rather than three degenerate quarks as in Figure 4. A nonzero m_s weakens those condensates which involve pairing between light and strange quarks. The CFL phase requires nonzero $\langle us \rangle$ and $\langle ds \rangle$ condensates; because these condensates pair quarks with differing Fermi momenta they can only exist if they are larger than of order $m_s^2/2\mu$, the difference between the u and s Fermi momenta in the absence of pairing. If one imagines increasing m_s at fixed μ , one finds a first order unlocking transition [7,8]:

⁷⁾ It turns out [5] that condensation in the color $\bar{\mathbf{3}}$ channel induces a condensate in the color $\mathbf{6}$ channel because this breaks no further symmetries [7]. The resulting condensates can be written in terms of κ_1 and κ_2 where $\langle \psi_L^{\alpha a} \psi_L^{\beta b} \rangle \sim \kappa_1 \delta^{\alpha a} \delta^{\beta b} + \kappa_2 \delta^{\alpha b} \delta^{\beta a}$. Here, the Kronecker δ ’s lock color and flavor rotations. The pure color $\bar{\mathbf{3}}$ condensate (2) has $\kappa_2 = -\kappa_1$.

⁸⁾ Once chiral symmetry is broken by color-flavor locking, there is no symmetry argument precluding the existence of an ordinary chiral condensate. Indeed, instanton effects do induce a nonzero $\langle \bar{q}q \rangle$ [5], but this is a small effect [44].

for larger m_s only u and d quarks pair and the 2SC phase is obtained. Conversely, as m_s is reduced in going from Figure 2 to 3 to 4, the region occupied by the CFL phase expands to encompass regions with smaller and smaller μ [7,8]. For any $m_s \neq \infty$, the CFL phase is the ground state at arbitrarily high density [7]. For larger values of m_s , there is a 2SC interlude on the horizontal axis, in which chiral symmetry is restored, before the CFL phase breaks it again at high densities. For smaller values of m_s , the possibility of quark-hadron continuity [6] as shown in Figure 4 arises. It should be noted that even when the strange and light quarks are not degenerate, the CFL phase may be continuous with a baryonic phase in which the densities of all the nucleons and hyperons are comparable; there are, however, phase transitions between this hypernuclear phase and ordinary nuclear matter [7].

The Nambu-Goldstone bosons in the CFL phase are Fermi surface excitations in which the orientation of the left-handed and right-handed diquark condensates oscillate out of phase in flavor space. The effective field theory describing these oscillations has been constructed [46,49,54]. Because the full theory is weakly coupled at asymptotically high densities, in this regime all coefficients in the effective theory describing the long wavelength meson physics are calculable from first principles. The decay constants $f_{\pi,K,\eta,\eta'}$ [49] and the meson masses $m_{\pi,K,\eta,\eta'}$ [49–53,55] are all now known. The meson masses depend on quark masses like $m^2 \sim m_q^2$ in the CFL phase (neglecting the small chiral condensate) [5], and their masses are inverted in the sense that the kaon is lighter than the pion [49]. The charged kaon mass $m_{K^\pm}^2 \sim m_d(m_u + m_s)\Delta/\mu$ is so light that it is likely less than the electron chemical potential, meaning that the CFL phase likely features a kaon condensate [58]. The dispersion relations describing the fermionic quasiparticle excitations in the CFL phase, which have the quantum numbers of an octet and a singlet of baryons, have also received attention [7,47]. So have the properties of the massive vector meson octet — the gluons which receive a mass via the Meissner-Anderson-Higgs mechanism [49,60,56]. We now have a description of the properties of the CFL phase and its excitations, in which much is known quantitatively if the value of the gap Δ is known. We describe estimates of Δ below.

It is interesting that both the 2SC and CFL phases satisfy anomaly matching constraints, even though it is not yet completely clear whether this must be the case when Lorentz invariance is broken by a nonzero density [61]. It is not yet clear how high density QCD with larger numbers of flavors [48] satisfies anomaly matching constraints. Also, anomaly matching in the 2SC phase requires that the up and down quarks of the third color remain ungapped; this requirement must, therefore, be modified once these quarks pair to form a $J = 1$ condensate, breaking rotational invariance [3].

Much effort has gone into estimating the magnitude of the gaps in the 2SC and CFL phases [2–5,7,8,18,20,44,62–77]. It would be ideal if this task were within the scope of lattice gauge theory as is, for example, the calculation of the critical temperature on the vertical axis of the phase diagram. Unfortunately, lattice methods relying on importance sampling have to this point been rendered exponentially impractical at nonzero baryon density by the complex action at nonzero

μ . There are more sophisticated algorithms which have allowed theories which are simpler than QCD but which have as severe a fermion sign problem as that in QCD at nonzero chemical potential to be simulated [78]. This bodes well for the future.⁹ Given the present absence of suitable lattice methods, the magnitude of the gaps in quark matter at large but accessible density has been estimated using two broad strategies. The first class of estimates are done within the context of models whose parameters are chosen to give reasonable vacuum physics. Examples include analyses in which the interaction between quarks is replaced simply by four-fermion interactions with the quantum numbers of the instanton interaction [3,4,18] or of one-gluon exchange [5,7], random matrix models [65], and more sophisticated analyses done using the instanton liquid model [20,44,84]. Renormalization group methods have also been used to explore the space of all possible effective four-fermion interactions [62,63]. These methods yield results which are in qualitative agreement: the favored condensates are as described above; the gaps range between several tens of MeV up to as large as about 100 MeV; the associated critical temperatures (above which the diquark condensates vanish) can be as large as about $T_c \sim 50$ MeV. This agreement between different models reflects the fact that what matters most is simply the strength of the attraction between quarks in the color $\mathbf{\bar{3}}$ channel, and by fixing the parameters of the model interaction to fit, say, the magnitude of the vacuum chiral condensate, one ends up with attractions of similar strengths in different models.

The second strategy for estimating gaps and critical temperatures is to use $\mu = \infty$ physics as a guide. At asymptotically large μ , models with short-range interactions are bound to fail because the dominant interaction is due to the long-range magnetic interaction coming from single-gluon exchange [42,66]. The collinear infrared divergence in small angle scattering via one-gluon exchange (which is regulated by dynamical screening [66]) results in a gap which is parametrically larger at $\mu \rightarrow \infty$ than it would be for any point-like four-fermion interaction. At $\mu \rightarrow \infty$, where $g(\mu) \rightarrow 0$, the gap takes the form [66]

$$\Delta \sim b\mu g(\mu)^{-5} \exp[-3\pi^2/\sqrt{2}g(\mu)] , \quad (3)$$

whereas for a point-like interaction with four-fermion coupling g^2 the gap goes like $\exp(-1/g^2)$. Son's result (3) has now been confirmed using a variety of methods [70,67–69,71,72,75]. The $\mathcal{O}(g^0)$ contribution to the prefactor b in (3) is not

⁹⁾ Note that quark pairing can be studied on the lattice in some models with four-fermion interactions and in two-color QCD [79]. The $N_c = 2$ case has also been studied analytically in Refs. [4,80]; pairing in this theory is simpler to analyze because quark Cooper pairs are color singlets. The $N_c \rightarrow \infty$ limit of QCD is often one in which hard problems become tractable. However, the ground state of $N_c = \infty$ QCD is a chiral density wave, not a color superconductor [81]. At asymptotically high densities color superconductivity persists up to N_c 's of order thousands [82,83] before being supplanted by the phase described in Ref. [81]. At any finite N_c , color superconductivity occurs at arbitrarily weak coupling whereas the chiral density wave does not. For $N_c = 3$, color superconductivity is still favored over the chiral density wave (although not by much) even if the interaction is so strong that the color superconductivity gap is $\sim \mu/2$ [84].

yet fully understood. It is estimated to be $b \sim 512\pi^4$ in the 2SC phase and $b \sim 512\pi^4 2^{-1/3} (2/3)^{5/2}$ in the CFL phase [70,67,69,71–73,48]. However, modifications to the quasiparticle dispersion relations in the normal (nonsuperconducting; high temperature) phase [71] and quasiparticle damping effects in the superconducting phase [77] both tend to reduce b . Also, the value of b is affected by the choice of the scale at which g is evaluated in (3). The results of Beane *et al.* demonstrate that g should be evaluated at a μ -dependent scale which is much lower than μ [75]. If, by convention, one instead takes g as $g(\mu)$, then b is significantly enhanced. Finally, examination of the gauge-dependent (and g -dependent) contributions to b in calculations based on the one-loop Schwinger-Dyson equation (e.g. those of Ref. [70,67,69,72]) reveals that they only begin to decrease for $g < 0.8$ [76]. This means that effects which have to date been neglected in all calculations (e.g. vertex corrections) are small corrections to b only for $\mu \gg 10^8$ MeV.

The phase of $N_c = 3$ QCD with nonzero isospin density ($\mu_I \neq 0$) and zero baryon density ($\mu = 0$) *can* be simulated on the lattice [85]. Although not physically realizable, it is very interesting to consider because phenomena arise which are similar to those occurring at large μ and, in this context, these phenomena can be analyzed on the lattice. In this setting, therefore, lattice simulations can be used to test calculational methods which have also been applied at large μ , where lattice simulation is unavailable. Large μ_I physics features large Fermi surfaces for down quarks and anti-up quarks, Cooper pairing of down and anti-up quarks, and a gap whose g -dependence is as in (3), albeit with a different coefficient of $1/g$ in the exponent [85]. This condensate has the same quantum numbers as the pion condensate expected at much lower μ_I , which means that a hypothesis of continuity between hadronic — in this case pionic — and quark matter as a function of μ_I can be tested on the lattice [85]. We henceforth return to the physically realizable setting in which differences between chemical potentials for different species of quarks (e.g. μ_I) are small compared to μ .

At large enough μ , the differences between u , d and s Fermi momenta decrease, while the result (3) demonstrates that the magnitude of the condensates *increases* slowly as $\mu \rightarrow \infty$. (As $\mu \rightarrow \infty$, the running coupling $g(\mu) \rightarrow 0$ logarithmically and the exponential factor in (3) goes to zero, but not sufficiently fast to overcome the growth of μ .) This means that the CFL phase is favored over the 2SC phase for $\mu \rightarrow \infty$ for any $m_s \neq \infty$ [7]. If we take the asymptotic estimates for the prefactor, quantitatively valid for $\mu \gg 10^8$ MeV [76], and apply them at accessible densities, say $\mu \sim 500$ MeV, it predicts gaps as large as about 100 MeV and critical temperatures as large as about 50 MeV [70]. Even though the asymptotic regime where Δ can be calculated from first principles with confidence is not accessed in nature, it is of great theoretical interest. The weak-coupling calculation of the gap in the CFL phase is the first step toward the weak-coupling calculation of other properties of this phase, in which chiral symmetry is broken and the spectrum of excitations is as in a confined phase. As we have described above, for example, the masses and decay constants of the pseudoscalar mesons can be calculated from first principles once Δ is known.

It is satisfying that two very different approaches, one using zero density phenomenology to normalize models, the other using weak-coupling methods valid at asymptotically high density, yield predictions for the gaps and critical temperatures at accessible densities which are in good agreement. Neither can be trusted quantitatively for quark number chemical potentials $\mu \sim 400 - 500$ MeV, as appropriate for the quark matter which may occur in compact stars. Still, both methods agree that the gaps at the Fermi surface are of order tens to 100 MeV, with critical temperatures about half as large.

$T_c \sim 50$ MeV is much larger relative to the Fermi momentum (say $\mu \sim 400 - 500$ MeV) than in low temperature superconductivity in metals. This reflects the fact that color superconductivity is induced by an attraction due to the primary, strong, interaction in the theory, rather than having to rely on much weaker secondary interactions, as in phonon mediated superconductivity in metals. Quark matter is a high- T_c superconductor by any reasonable definition. It is unfortunate that its T_c is nevertheless low enough that it is unlikely the phenomenon can be realized in heavy ion collisions.

IV COLOR SUPERCONDUCTIVITY IN COMPACT STARS

Our current understanding of the color superconducting state of quark matter leads us to believe that it may occur naturally in compact stars. The critical temperature T_c below which quark matter is a color superconductor is high enough that any quark matter which occurs within neutron stars that are more than a few seconds old is in a color superconducting state. In the absence of lattice simulations, present theoretical methods are not accurate enough to determine whether neutron star cores are made of hadronic matter or quark matter. They also cannot determine whether any quark matter which arises will be in the CFL or 2SC phase: the difference between the u , d and s Fermi momenta will be a few tens of MeV which is comparable to estimates of the gap Δ ; the CFL phase occurs when Δ is large compared to all differences between Fermi momenta. Just as the higher temperature regions of the QCD phase diagram are being mapped out in heavy ion collisions, we need to learn how to use neutron star phenomena to determine whether they feature cores made of 2SC quark matter, CFL quark matter or hadronic matter, thus teaching us about the high density region of the QCD phase diagram. It is therefore important to look for astrophysical consequences of color superconductivity.

Equation of State: Much of the work on the consequences of quark matter within a compact star has focussed on the effects of quark matter on the equation of state, and hence on the radius of the star. As a Fermi surface phenomenon, color superconductivity has little effect on the equation of state: the pressure is an integral over the whole Fermi volume. Color superconductivity modifies the equation of state at the $\sim (\Delta/\mu)^2$ level, typically by a few percent [3]. Such

small effects can be neglected in present calculations, and for this reason I will not attempt to survey the many ways in which observations of neutron stars are being used to constrain the equation of state [86].

I will describe one current idea, however. As a neutron star in a low mass X-ray binary (LMXB) is spun up by accretion from its companion, it becomes more oblate and its central density decreases. If it contains a quark matter core, the volume fraction occupied by this core decreases, the star expands, and its moment of inertia increases. This raises the possibility [87] of a period during the spin-up history of an LMXB when the neutron star is gaining angular momentum via accretion, but is gaining sufficient moment of inertia that its angular frequency is hardly increasing. In their modelling of this effect, Glendenning and Weber [87] discover that LMXB's should spend a significant fraction of their history with a frequency of around 200 Hz, while their quark cores are being spun out of existence, before eventually spinning up to higher frequencies. This may explain the observation that LMXB frequencies are clustered around 250-350 Hz [88], which is otherwise puzzling in that it is thought that LMXB's provide the link between canonical pulsars and millisecond pulsars, which have frequencies as large as 600 Hz [89]. It will be interesting to see how robust the result of Ref. [87] is to changes in model assumptions and also how its predictions fare when compared to those of other explanations which posit upper bounds on LMXB frequencies [90], rather than a most probable frequency range with no associated upper bound [87]. We note here that because Glendenning and Weber's effect depends only on the equation of state and not on other properties of quark matter, the fact that the quark matter must in fact be a color superconductor will not affect the results in any significant way. If Glendenning and Weber's explanation for the observed clustering of LMXB frequencies proves robust, it would imply that pulsars with lower rotational frequencies feature quark matter cores.

Cooling by Neutrino Emission: We turn now to neutron star phenomena which *are* affected by Fermi surface physics. For the first 10^{5-6} years of its life, the cooling of a neutron star is governed by the balance between heat capacity and the loss of heat by neutrino emission. How are these quantities affected by the presence of a quark matter core? This has been addressed recently in Refs. [91,92], following earlier work in Ref. [93]. Both the specific heat C_V and the neutrino emission rate L_ν are dominated by physics within T of the Fermi surface. If, as in the CFL phase, all quarks have a gap $\Delta \gg T$ then the contribution of quark quasiparticles to C_V and L_ν is suppressed by $\sim \exp(-\Delta/T)$. There may be other contributions to L_ν [91], but these are also very small. The specific heat is dominated by that of the electrons, although it may also receive a small contribution from the CFL phase Goldstone bosons. Although further work is required, it is already clear that both C_V and L_ν are much smaller than in the nuclear matter outside the quark matter core. This means that the total heat capacity and the total neutrino emission rate (and hence the cooling rate) of a neutron star with a CFL core will be determined completely by the nuclear matter outside the core. The quark matter core is “inert”: with its small heat capacity and emission rate it has little influence

on the temperature of the star as a whole. As the rest of the star emits neutrinos and cools, the core cools by conduction, because the electrons keep it in good thermal contact with the rest of the star. These qualitative expectations are nicely borne out in the calculations presented by Page et al. [92].

The analysis of the cooling history of a neutron star with a quark matter core in the 2SC phase is more complicated. The red and green up and down quarks pair with a gap many orders of magnitude larger than the temperature, which is of order 10 keV, and are therefore inert as described above. Any strange quarks present will form a $\langle ss \rangle$ condensate with angular momentum $J = 1$ which locks to color in such a way that rotational invariance is not broken [94]. The resulting gap has been estimated to be of order hundreds of keV [94], although applying results of Ref. [95] suggests a somewhat smaller gap, around 10 keV. The blue up and down quarks can also pair, forming a $J = 1$ condensate which breaks rotational invariance [3]. The related gap was estimated to be a few keV [3], but this estimate was not robust and should be revisited in light of more recent developments given its importance in the following. The critical temperature T_c above which no condensate forms is of order the zero-temperature gap Δ . ($T_c = 0.57\Delta$ for $J = 0$ condensates [67].) Therefore, if there are quarks for which $\Delta \sim T$ or smaller, these quarks do not pair at temperature T . Such quark quasiparticles will radiate neutrinos rapidly (via direct URCA reactions like $d \rightarrow u + e + \bar{\nu}$, $u \rightarrow d + e^+ + \nu$, etc.) and the quark matter core will cool rapidly and determine the cooling history of the star as a whole [93,92]. The star will cool rapidly until its interior temperature is $T < T_c \sim \Delta$, at which time the quark matter core will become inert and the further cooling history will be dominated by neutrino emission from the nuclear matter fraction of the star. If future data were to show that neutron stars first cool rapidly (direct URCA) and then cool more slowly, such data would allow an estimate of the smallest quark matter gap. We are unlikely to be so lucky. The simple observation of rapid cooling would *not* be an unambiguous discovery of quark matter with small gaps; there are other circumstances in which the direct URCA processes occurs. However, if as data on neutron star temperatures improves in coming years the standard cooling scenario proves correct, indicating the absence of the direct URCA processes, this *would* rule out the presence of quark matter with gaps in the 10 keV range or smaller. The presence of a quark matter core in which all gaps are $\gg T$ can never be revealed by an analysis of the cooling history.

Supernova Neutrinos: We now turn from neutrino emission from a neutron star which is many years old to that from the protoneutron star during the first seconds of a supernova. Carter and Reddy [96] have pointed out that when this protoneutron star is heated up to its maximum temperature of order 30-50 MeV, it may feature a quark matter core which is too hot for color superconductivity. As the core of the protoneutron star cools over the coming seconds, if it contains quark matter this quark matter will cool through T_c , entering the color superconducting regime of the QCD phase diagram from above. For $T \sim T_c$, the specific heat rises and the cooling slows. Then, as T drops further and Δ increases to become greater than T , the specific heat drops rapidly. Furthermore, as the number density of

quark quasiparticles becomes suppressed by $\exp(-\Delta/T)$, the neutrino transport mean free path rapidly becomes very long [96]. This means that all the neutrinos previously trapped in the now color superconducting core are able to escape in a sudden burst. If we are lucky enough that a terrestrial neutrino detector sees thousands of neutrinos from a future supernova, Carter and Reddy’s results suggest that there may be a signature of the transition to color superconductivity present in the time distribution of these neutrinos. Neutrinos from the core of the protoneutron star will lose energy as they scatter on their way out, but because they will be the last to reach the surface of last scattering, they will be the final neutrinos received at the earth. If they are emitted from the quark matter core in a sudden burst, they may therefore result in a bump at late times in the temporal distribution of the detected neutrinos. More detailed study remains to be done in order to understand how Carter and Reddy’s signature, dramatic when the neutrinos escape from the core, is processed as the neutrinos traverse the rest of the protoneutron star and reach their surface of last scattering.

R-mode Instabilities: Another arena in which color superconductivity comes into play is the physics of r-mode instabilities. A neutron star whose angular rotation frequency Ω is large enough is unstable to the growth of r-mode oscillations which radiate away angular momentum via gravitational waves, reducing Ω . What does “large enough” mean? The answer depends on the damping mechanisms which act to prevent the growth of the relevant modes. Both shear viscosity and bulk viscosity act to damp the r-modes, preventing them from going unstable. The bulk viscosity and the quark contribution to the shear viscosity both become exponentially small in quark matter with $\Delta > T$ and as a result, as Madsen [97] has shown, a compact star made *entirely* of quark matter with gaps $\Delta = 1$ MeV or greater is unstable if its spin frequency is greater than tens to 100 Hz. Many compact stars spin faster than this, and Madsen therefore argues that compact stars cannot be strange quark stars unless some quarks remain ungapped. Alas, this powerful argument becomes much less powerful in the context of a neutron star with a quark matter core. First, the r-mode oscillations have a wave form whose amplitude is largest at large radius, outside the core. Second, in an ordinary neutron star there is a new source of damping: friction at the boundary between the crust and the neutron superfluid “mantle” keeps the r-modes stable regardless of the properties of a quark matter core [98,97].

Magnetic Field Evolution: Next, we turn to the physics of magnetic fields within color superconducting neutron star cores [99,100]. The interior of a conventional neutron star is a superfluid (because of neutron-neutron pairing) and is an electromagnetic superconductor (because of proton-proton pairing). Ordinary magnetic fields penetrate it only in the cores of magnetic flux tubes. A color superconductor behaves differently. At first glance, it seems that because a diquark Cooper pair has nonzero electric charge, a diquark condensate must exhibit the standard Meissner effect, expelling ordinary magnetic fields or restricting them to flux tubes within whose cores the condensate vanishes. This is not the case [100]. In both the 2SC and CFL phase a linear combination of the $U(1)$ gauge transforma-

tion of ordinary electromagnetism and one (the eighth) color gauge transformation remains unbroken even in the presence of the condensate. This means that the ordinary photon A_μ and the eighth gluon G_μ^8 are replaced by new linear combinations

$$\begin{aligned} A_\mu^{\tilde{Q}} &= \cos \alpha_0 A_\mu + \sin \alpha_0 G_\mu^8 \\ A_\mu^X &= -\sin \alpha_0 A_\mu + \cos \alpha_0 G_\mu^8 \end{aligned} \quad (4)$$

where $A_\mu^{\tilde{Q}}$ is massless and A_μ^X is massive. That is, $B_{\tilde{Q}}$ satisfies the ordinary Maxwell equations while B_X experiences a Meissner effect. The mixing angle α_0 is the analogue of the Weinberg angle in electroweak theory, in which the presence of the Higgs condensate causes the A_μ^Y and the third $SU(2)_W$ gauge boson to mix to form the photon, A_μ , and the massive Z boson. $\sin(\alpha_0)$ is proportional to e/g and turns out to be about $1/20$ in the 2SC phase and $1/40$ in the CFL phase [100]. This means that the \tilde{Q} -photon which propagates in color superconducting quark matter is mostly photon with only a small gluon admixture. If a color superconducting neutron star core is subjected to an ordinary magnetic field, it will either expel the X component of the flux or restrict it to flux tubes, but it can (and does [100]) admit the great majority of the flux in the form of a $B_{\tilde{Q}}$ magnetic field satisfying Maxwell's equations. The decay in time of this “free field” (i.e. not in flux tubes) is limited by the \tilde{Q} -conductivity of the quark matter. A color superconductor is not a \tilde{Q} -superconductor — that is the whole point — but it turns out to be a very good \tilde{Q} -conductor due to the presence of electrons: the $B_{\tilde{Q}}$ magnetic field decays only on a time scale which is much longer than the age of the universe [100]. This means that a quark matter core within a neutron star serves as an “anchor” for the magnetic field: whereas in ordinary nuclear matter the magnetic flux tubes can be dragged outward by the neutron superfluid vortices as the star spins down [101], the magnetic flux within the color superconducting core simply cannot decay. Even though this distinction is a qualitative one, it will be difficult to confront it with data since what is observed is the total dipole moment of the neutron star. A color superconducting core anchors those magnetic flux lines which pass through the core, while in a neutron star with no quark matter core the entire internal magnetic field can decay over time. In both cases, however, the total dipole moment can change since the magnetic flux lines which do not pass through the core can move.

Glitches in Quark Matter: The final consequence of color superconductivity we wish to discuss is the possibility that (some) glitches may originate within quark matter regions of a compact star [95]. In any context in which color superconductivity arises in nature, it is likely to involve pairing between species of quarks with differing chemical potentials. If the chemical potential difference is small enough, BCS pairing occurs as we have been discussing. If the Fermi surfaces are too far apart, no pairing between the species is possible. The transition between the BCS and unpaired states as the splitting between Fermi momenta increases has been studied in electron [102] and QCD [7,8,103] superconductors, assuming that no other state intervenes. However, there is good reason to think that another state can occur. This is the “LOFF” state, first explored by Larkin and Ovchinnikov [104]

and Fulde and Ferrell [105] in the context of electron superconductivity in the presence of magnetic impurities. They found that near the unpairing transition, it is favorable to form a state in which the Cooper pairs have nonzero momentum. This is favored because it gives rise to a region of phase space where each of the two quarks in a pair can be close to its Fermi surface, and such pairs can be created at low cost in free energy. Condensates of this sort spontaneously break translational and rotational invariance, leading to gaps which vary periodically in a crystalline pattern. If in some shell within the quark matter core of a neutron star (or within a strange quark star) the quark number densities are such that crystalline color superconductivity arises, rotational vortices may be pinned in this shell, making it a locus for glitch phenomena.

We [95] have explored the range of parameters for which crystalline color superconductivity occurs in the QCD phase diagram, upon making various simplifying assumptions. For example, we focus primarily on a four-fermion interaction with the quantum numbers of single gluon exchange. Also, we only consider pairing between u and d quarks, with $\mu_d = \bar{\mu} + \delta\mu$ and $\mu_u = \bar{\mu} - \delta\mu$, whereas we expect a LOFF state when the difference between the Fermi momenta of any two quark flavors is near an unpairing transition. We find the LOFF state is favored for values of $\delta\mu$ which satisfy $\delta\mu_1 < \delta\mu < \delta\mu_2$ where $\delta\mu_1/\Delta_0 = 0.707$ and $\delta\mu_2/\Delta_0 = 0.754$ in the weak coupling limit in which $\Delta_0 \ll \mu$. (Here, Δ_0 is the 2SC gap that would arise if $\delta\mu$ were zero.) The LOFF gap parameter decreases from $0.23\Delta_0$ at $\delta\mu = \delta\mu_1$ (where there is a first order BCS-LOFF phase transition) to zero at $\delta\mu = \delta\mu_2$ (where there is a second order LOFF-normal transition). Except for very close to $\delta\mu_2$, the critical temperature above which the LOFF state melts will be much higher than typical neutron star temperatures. At stronger coupling the LOFF gap parameter decreases relative to Δ_0 and the window of $\delta\mu/\Delta_0$ within which the LOFF state is favored shrinks. The window grows if the interaction is changed to weight electric gluon exchange more heavily than magnetic gluon exchange.

The quark matter which may be present within a compact star will be in the crystalline color superconductor (LOFF) state if $\delta\mu/\Delta_0$ is in the requisite range. For a reasonable value of $\delta\mu$, say 25 MeV, this occurs if the gap Δ_0 which characterizes the uniform color superconductor present at smaller values of $\delta\mu$ is about 40 MeV. This is in the middle of the range of present estimates. Both $\delta\mu$ and Δ_0 vary as a function of density and hence as a function of radius in a compact star. Although it is too early to make quantitative predictions, the numbers are such that crystalline color superconducting quark matter may very well occur in a range of radii within a compact star. It is therefore worthwhile to consider the consequences.

Many pulsars have been observed to glitch. Glitches are sudden jumps in rotation frequency Ω which may be as large as $\Delta\Omega/\Omega \sim 10^{-6}$, but may also be several orders of magnitude smaller. The frequency of observed glitches is statistically consistent with the hypothesis that all radio pulsars experience glitches [106]. Glitches are thought to originate from interactions between the rigid crust, somewhat more than a kilometer thick in a typical neutron star, and rotational vortices in the neutron superfluid which are moving (or trying to move) outward as the star spins

down. Although the models [107] differ in important respects, all agree that the fundamental requirements are the presence of rotational vortices in a superfluid and the presence of a rigid structure which impedes the motion of vortices and which encompasses enough of the volume of the pulsar to contribute significantly to the total moment of inertia.

Although it is premature to draw quantitative conclusions, it is interesting to speculate that some glitches may originate deep within a pulsar which features a quark matter core, in a region of that core in which the color superconducting quark matter is in a LOFF crystalline color superconductor phase. A three flavor analysis is required to determine whether the LOFF phase is a superfluid. If the only pairing is between u and d quarks, this 2SC phase is not a superfluid [3,7], whereas if all three quarks pair in some way, a superfluid *is* obtained [5,7]. Henceforth, we suppose that the LOFF phase is a superfluid, which means that if it occurs within a pulsar it will be threaded by an array of rotational vortices. It is reasonable to expect that these vortices will be pinned in a LOFF crystal, in which the diquark condensate varies periodically in space. Indeed, one of the suggestions for how to look for a LOFF phase in terrestrial electron superconductors relies on the fact that the pinning of magnetic flux tubes (which, like the rotational vortices of interest to us, have normal cores) is expected to be much stronger in a LOFF phase than in a uniform BCS superconductor [108].

A real calculation of the pinning force experienced by a vortex in a crystalline color superconductor must await the determination of the crystal structure of the LOFF phase. We can, however, attempt an order of magnitude estimate along the same lines as that done by Anderson and Itoh [109] for neutron vortices in the inner crust of a neutron star. In that context, this estimate has since been made quantitative [110,111,107]. For one specific choice of parameters [95], the LOFF phase is favored over the normal phase by a free energy $F_{\text{LOFF}} \sim 5 \times (10 \text{ MeV})^4$ and the spacing between nodes in the LOFF crystal is $b = \pi/(2|\mathbf{q}|) \sim 9 \text{ fm}$. The thickness of a rotational vortex is given by the correlation length $\xi \sim 1/\Delta \sim 25 \text{ fm}$. The pinning energy is the difference between the energy of a section of vortex of length b which is centered on a node of the LOFF crystal vs. one which is centered on a maximum of the LOFF crystal. It is of order $E_p \sim F_{\text{LOFF}} b^3 \sim 4 \text{ MeV}$. The resulting pinning force per unit length of vortex is of order $f_p \sim E_p/b^2 \sim (4 \text{ MeV})/(80 \text{ fm}^2)$. A complete calculation will be challenging because $b < \xi$, and is likely to yield an f_p which is somewhat less than that we have obtained by dimensional analysis. Note that our estimate of f_p is quite uncertain both because it is only based on dimensional analysis and because the values of Δ , b and F_{LOFF} are uncertain. (We have a good understanding of all the ratios Δ/Δ_0 , $\delta\mu/\Delta_0$, q/Δ_0 and consequently $b\Delta_0$ in the LOFF phase. It is of course the value of the BCS gap Δ_0 which is uncertain.) It is premature to compare our crude result to the results of serious calculations of the pinning of crustal neutron vortices as in Refs. [110,111,107]. It is nevertheless remarkable that they prove to be similar: the pinning energy of neutron vortices in the inner crust is $E_p \approx 1 - 3 \text{ MeV}$ and the pinning force per unit length is $f_p \approx (1 - 3 \text{ MeV})/(200 - 400 \text{ fm}^2)$. Perhaps,

therefore, glitches occurring in a region of crystalline color superconducting quark matter may yield similar phenomenology to those occurring in the inner crust.

Perhaps the most interesting consequence of these speculations arises in the context of compact stars made entirely of strange quark matter. The work of Witten [112] and Farhi and Jaffe [113] raised the possibility that strange quark matter may be energetically stable relative to nuclear matter even at zero pressure. If this is the case it raises the question whether observed compact stars—pulsars, for example—are strange quark stars [114,115] rather than neutron stars. A conventional neutron star may feature a core made of strange quark matter, as we have been discussing above.¹⁰ Strange quark stars, on the other hand, are made (almost) entirely of quark matter with either no hadronic matter content at all or with a thin crust, of order one hundred meters thick, which contains no neutron superfluid [115,116]. The nuclei in this thin crust are supported above the quark matter by electrostatic forces; these forces cannot support a neutron fluid. Because of the absence of superfluid neutrons, and because of the thinness of the crust, no successful models of glitches in the crust of a strange quark star have been proposed. Since pulsars are observed to glitch, the apparent lack of a glitch mechanism for strange quark stars has been the strongest argument that pulsars cannot be strange quark stars [117–119]. This conclusion must now be revisited.

Madsen’s conclusion [97] that a strange quark star is prone to r-mode instability due to the absence of damping must also be revisited, since the relevant fluid oscillations may be damped within or at the boundary of a region of crystalline color superconductor.

The quark matter in a strange quark star, should one exist, would be a color superconductor. Depending on the mass of the star, the quark number densities increase by a factor of about two to ten in going from the surface to the center [115]. This means that the chemical potential differences among the three quarks will vary also, and there could be a range of radii within which the quark matter is in a crystalline color superconductor phase. This raises the possibility of glitches in strange quark stars. Because the variation in density with radius is gradual, if a shell of LOFF quark matter exists it need not be particularly thin. And, we have seen, the pinning forces may be comparable in magnitude to those in the inner crust of a conventional neutron star. It has recently been suggested (for reasons unrelated to our considerations) that certain accreting compact stars may be strange quark stars [120], although the evidence is far from unambiguous [121]. In contrast, it has been thought that, because they glitch, conventional radio pulsars cannot be strange quark stars. Our work questions this assertion by raising the possibility that glitches may originate within a layer of quark matter which is in a crystalline color superconducting state.

¹⁰⁾ Note that a convincing discovery of a quark matter core within an otherwise hadronic neutron star would demonstrate conclusively that strange quark matter is *not* stable at zero pressure, thus ruling out the existence of strange quark stars. It is not possible for neutron stars with quark matter cores and strange quark stars to both be stable.

Closing Remarks: The answer to the question of whether the QCD phase diagram does or does not feature a 2SC interlude on the horizontal axis, separating the CFL and baryonic phases in both of which chiral symmetry is broken, depends on whether the strange quark is effectively heavy or effectively light. This is the central outstanding qualitative question about the high density region of the QCD phase diagram. A central question at higher temperatures, namely where does nature locate the critical point E , also depends on the strange quark mass. Both questions are hard to answer theoretically with any confidence. The high temperature region is in better shape, however, because the program of experimentation described in Section II allows heavy ion collision experiments to search for the critical point E . Theorists have described how to use phenomena characteristic of freezeout in its vicinity to discover E ; this gives experimentalists the ability to locate it convincingly. The discovery of E would allow us to draw the higher temperature regions of the map of the QCD phase diagram in ink. At high density, there has been much recent progress in our understanding of how the presence of color superconducting quark matter in a compact star would affect five different phenomena: cooling by neutrino emission, the temporal pattern of the neutrinos emitted by a supernova, the evolution of neutron star magnetic fields, r-mode instabilities, and glitches. Nevertheless, much theoretical work remains to be done before we can make sharp proposals for which astrophysical observations are most likely to help teach us how to ink in the boundaries of the 2SC and CFL regions in the QCD phase diagram. Best of all, though, and as in heavy ion physics, a wealth of new data is expected over the next few years.

REFERENCES

1. B. Barrois, Nucl. Phys. **B129**, 390 (1977); S. Frautschi, Proceedings of workshop on hadronic matter at extreme density, Erice 1978; B. Barrois, “Nonperturbative effects in dense quark matter”, Cal Tech PhD thesis, UMI 79-04847-mc (1979).
2. D. Bailin and A. Love, Phys. Rept. **107**, 325 (1984), and references therein.
3. M. Alford, K. Rajagopal and F. Wilczek, Phys. Lett. **B422**, 247 (1998) [hep-ph/9711395].
4. R. Rapp, T. Schäfer, E. V. Shuryak and M. Velkovsky, Phys. Rev. Lett. **81**, 53 (1998) [hep-ph/9711396].
5. M. Alford, K. Rajagopal and F. Wilczek, Nucl. Phys. **B537**, 443 (1999) [hep-ph/9804403].
6. T. Schäfer and F. Wilczek, Phys. Rev. Lett. **82**, 3956 (1999) [hep-ph/9811473].
7. M. Alford, J. Berges and K. Rajagopal, Nucl. Phys. **B558**, 219 (1999) [hep-ph/9903502].
8. T. Schäfer and F. Wilczek, Phys. Rev. **D60**, 074014 (1999) [hep-ph/9903503].
9. M. Stephanov, K. Rajagopal and E. Shuryak, Phys. Rev. Lett. **81**, 4816 (1998) [hep-ph/9806219].
10. M. Stephanov, K. Rajagopal and E. Shuryak, Phys. Rev. **D60**, 114028 (1999) [hep-ph/9903292].

11. For a longer review, see K. Rajagopal, in Quark-Gluon Plasma 2, (World Scientific, 1995) 484, ed. R. Hwa [hep-ph/9504310].
12. R. Pisarski and F. Wilczek, Phys. Rev. **D29**, 338 (1984); F. Wilczek, Int. J. Mod. Phys. **A7**, 3911 (1992); K. Rajagopal and F. Wilczek, Nucl. Phys. **B399**, 395 (1993).
13. For reviews, see F. Karsch, hep-lat/9909006; E. Laermann Nucl. Phys. Proc. Suppl. **63**, 114 (1998); and A. Ukawa, Nucl. Phys. Proc. Suppl. **53**, 106 (1997).
14. A. Ali Khan *et al*, [CP-PACS Collaboration], hep-lat/0008011.
15. For example, S. Gottlieb *et al.*, Phys. Rev. **D55**, 6852 (1997); F. Karsch, hep-lat/9909006.
16. A. Barducci, R. Casalbuoni, S. DeCurtis, R. Gatto, G. Pettini, Phys. Lett. **B231**, 463 (1989); S.P. Klevansky, Rev. Mod. Phys. **64**, 649 (1992); A. Barducci, R. Casalbuoni, G. Pettini and R. Gatto, Phys. Rev. **D49**, 426 (1994).
17. M. Stephanov, Phys. Rev. Lett. **76**, 4472 (1996); Nucl. Phys. Proc. Suppl. **53**, 469 (1997).
18. J. Berges and K. Rajagopal, Nucl. Phys. **B538**, 215 (1999) [hep-ph/9804233].
19. M. A. Halasz, A. D. Jackson, R. E. Shrock, M. A. Stephanov and J. J. Verbaarschot, Phys. Rev. **D58**, 096007 (1998) [hep-ph/9804290].
20. G. W. Carter and D. Diakonov, Phys. Rev. **D60**, 016004 (1999) [hep-ph/9812445].
21. For a review, see I. Lawrie and S. Sarbach in Phase Transitions and Critical Phenomena **9**, 1 (Academic Press, 1984), ed. C. Domb and J. Lebowitz.
22. F. Wilczek, Int. J. Mod. Phys. **A7**, 3911 (1992); K. Rajagopal and F. Wilczek, Nucl. Phys. **B399**, 395 (1993).
23. F. Brown *et al*, Phys. Rev. Lett. **65**, 2491 (1990).
24. JLQCD Collaboration, Nucl. Phys. Proc. Suppl. **73**, 459 (1999).
25. Y. Iwasaki *et al*, Phys. Rev. **D54**, 7010 (1996).
26. See, e.g., P. Braun-Munzinger, J. Stachel, J. P. Wessels and N. Xu, Phys. Lett. **B344**, 43 (1994); *ibid.* **B365**, 1 (1996); P. Braun-Munzinger and J. Stachel, Nucl. Phys. **A638**, 3 (1998).
27. B. B. Back *et al*, [PHOBOS Collaboration], to appear in Phys. Rev. Lett., hep-ex/0007036.
28. H. Appelshauser *et al.* [NA49 Collaboration], Phys. Lett. **B459**, 679 (1999).
29. G. Baym and H. Heiselberg, Phys. Lett. **B469**, 7 (1999).
30. G. Danilov and E. Shuryak, nucl-th/9908027.
31. A. Bialas and V. Koch, Phys. Lett. **B456**, 1 (1999).
32. St. Mrówczyński, Phys. Lett. **B430**, 9 (1998).
33. B. Berdnikov and K. Rajagopal, Phys. Rev. **D61**, 105017 (2000) [hep-ph/9912274].
34. P. C. Hohenberg and B. I. Halperin, Rev. Mod. Phys. **49**, 435 (1977).
35. E. Schnedermann and U. Heinz, Phys. Rev. **C47**, 1738 (1993); and **C50**, 1675 (1994); C. M. Hung and E. Shuryak, Phys. Rev. **C57**, 1891 (1998); B. Tomasik, U. A. Wiedemann and U. Heinz, nucl-th/9907096; L. V. Bravina *et al*, Phys. Rev. **C60**, 024904 (1999).
36. W. H. Zurek, Nature **317**, 505 (1985); Phys. Rept. **276**, 177 (1996).
37. N. D. Antunes, L. M. A. Bettencourt and W. H. Zurek, Phys. Rev. Lett. **82**, 2824 (1999), and references therein.

38. I. Chuang, R. Durrer, N. Turok and B. Yurke, *Science* **251**, 1336 (1991); M. J. Bowick, L. Chander, E. A. Schiff and A. M. Srivastava, *ibid.* **263**, 943 (1994).
39. C. Bäuerle *et al.*, *Nature* **382**, 332 (1996); V. M. H. Ruutu *et al.*, *Nature* **382**, 334 (1996); *Phys. Rev. Lett.* **80**, 1465 (1998); V. B. Eltsov, M. Krusius and G. E. Volovik, *cond-mat/9809125*.
40. D. Boyanovsky, H. J. de Vega and M. Simionato, *hep-ph/0004159*.
41. Reviewed in U. Heinz and M. Jacob, *nucl-th/0002042*.
42. R. D. Pisarski and D. H. Rischke, *Phys. Rev. Lett.* **83**, 37 (1999) [*nucl-th/9811104*].
43. R. D. Pisarski, *Phys. Rev.* **C62**, 035202 (2000) [*nucl-th/9912070*].
44. R. Rapp, T. Schäfer, E. V. Shuryak and M. Velkovsky, *Annals Phys.* **280**, 35 (2000) [*hep-ph/9904353*].
45. D. K. Hong, M. Rho and I. Zahed, *Phys. Lett.* **B468**, 261 (1999) [*hep-ph/9906551*].
46. R. Casalbuoni and R. Gatto, *Phys. Lett.* **B464**, 111 (1999) [*hep-ph/9908227*].
47. M. Alford, J. Berges and K. Rajagopal, *Phys. Rev. Lett.* **84**, 598 (2000) [*hep-ph/9908235*].
48. T. Schäfer, *Nucl. Phys.* **B575**, 269 (2000) [*hep-ph/9909574*].
49. D. T. Son and M. A. Stephanov, *Phys. Rev.* **D61**, 074012 (2000) [*hep-ph/9910491*]; erratum, *ibid.* **D62**, 059902 (2000) [*hep-ph/0004095*].
50. M. Rho, A. Wirzba and I. Zahed, *Phys. Lett.* **B473**, 126 (2000) [*hep-ph/9910550*].
51. D. K. Hong, T. Lee and D. Min, *Phys. Lett.* **B477**, 137 (2000) [*hep-ph/9912531*].
52. C. Manuel and M. H. Tytgat, *Phys. Lett.* **B479**, 190 (2000) [*hep-ph/0001095*].
53. M. Rho, E. Shuryak, A. Wirzba and I. Zahed, *Nucl. Phys.* **A676**, 273 (2000) [*hep-ph/0001104*].
54. K. Zarembo, *Phys. Rev.* **D62**, 054003 (2000) [*hep-ph/0002123*].
55. S. R. Beane, P. F. Bedaque and M. J. Savage, *Phys. Lett.* **B483**, 131 (2000) [*hep-ph/0002209*].
56. D. H. Rischke, *Phys. Rev.* **D62**, 054017 (2000) [*nucl-th/0003063*].
57. D. K. Hong, *hep-ph/0006105*.
58. T. Schäfer, *nucl-th/0007021*.
59. M. A. Nowak, M. Rho, A. Wirzba and I. Zahed, *hep-ph/0007034*.
60. D. H. Rischke, *Phys. Rev.* **D62**, 034007 (2000) [*nucl-th/0001040*]; G. Carter and D. Diakonov, *Nucl. Phys.* **B582**, 571 (2000) [*hep-ph/0001318*].
61. F. Sannino, *Phys. Lett.* **B480**, 280 (2000) [*hep-ph/0002277*]; R. Casalbuoni, Z. Duan and F. Sannino, *hep-ph/0004207*; S. D. Hsu, F. Sannino and M. Schwetz, *hep-ph/0006059*.
62. N. Evans, S. D. H. Hsu and M. Schwetz, *Nucl. Phys.* **B551**, 275 (1999) [*hep-ph/9808444*]; *Phys. Lett.* **B449**, 281 (1999) [*hep-ph/9810514*].
63. T. Schäfer and F. Wilczek, *Phys. Lett.* **B450**, 325 (1999) [*hep-ph/9810509*].
64. N. O. Agasian, B. O. Kerbikov and V. I. Shevchenko, *Phys. Rept.* **320**, 131 (1999) [*hep-ph/9902335*].
65. B. Vanderheyden and A. D. Jackson, *hep-ph/0003150*.
66. D. T. Son, *Phys. Rev.* **D59**, 094019 (1999) [*hep-ph/9812287*].
67. R. D. Pisarski and D. H. Rischke, *Phys. Rev.* **D60**, 094013 (1999) [*nucl-th/9903023*]; *Phys. Rev.* **D61**, 051501 (2000) [*nucl-th/9907041*]; *Phys. Rev.* **D61**, 074017 (2000) [*nucl-th/9910056*];

68. D. K. Hong, Phys. Lett. **B473**, 118 (2000) [hep-ph/9812510]; Nucl. Phys. **B582**, 451 (2000) [hep-ph/9905523].
69. D. K. Hong, V. A. Miransky, I. A. Shovkovy and L. C. Wijewardhana, Phys. Rev. **D61**, 056001 (2000), erratum *ibid.* **D62**, 059903 (2000) [hep-ph/9906478].
70. T. Schäfer and F. Wilczek, Phys. Rev. **D60**, 114033 (1999) [hep-ph/9906512].
71. W. E. Brown, J. T. Liu and H. Ren, Phys. Rev. **D61**, 114012 (2000) [hep-ph/9908248]; Phys. Rev. **D62**, 054016 (2000) [hep-ph/9912409]; Phys. Rev. **D62**, 054013 (2000) [hep-ph/0003199].
72. S. D. Hsu and M. Schwetz, Nucl. Phys. **B572**, 211 (2000) [hep-ph/9908310].
73. I. A. Shovkovy and L. C. Wijewardhana, Phys. Lett. **B470**, 189 (1999) [hep-ph/9910225].
74. N. Evans, J. Hormuzdiar, S. D. Hsu and M. Schwetz, Nucl. Phys. **B581**, 391 (2000) [hep-ph/9910313].
75. S. R. Beane, P. F. Bedaque and M. J. Savage, nucl-th/0004013.
76. K. Rajagopal and E. Shuster, hep-ph/0004074.
77. C. Manuel, hep-ph/0005040.
78. S. Chandrasekharan and U. Wiese, Phys. Rev. Lett. **83**, 3116 (1999) [cond-mat/9902128].
79. UKQCD Collaboration, Phys. Rev. **D59** (1999) 116002; S. Hands, J. B. Kogut, M. Lombardo and S. E. Morrison, Nucl. Phys. **B558**, 327 (1999) [hep-lat/9902034]; S. Hands, I. Montvay, S. Morrison, M. Oevers, L. Scorzato and J. Skullerud, hep-lat/0006018.
80. J. B. Kogut, M. A. Stephanov and D. Toublan, Phys. Lett. **B464**, 183 (1999) [hep-ph/9906346]; J. B. Kogut, M. A. Stephanov, D. Toublan, J. J. Verbaarschot and A. Zhitnitsky, Nucl. Phys. **B582**, 477 (2000) [hep-ph/0001171].
81. D. V. Deryagin, D. Yu. Grigoriev and V. A. Rubakov, Int. J. Mod. Phys. **A7**, 659 (1992).
82. E. Shuster and D. T. Son, Nucl. Phys. **B573**, 434 (2000) [hep-ph/9905448].
83. B. Park, M. Rho, A. Wirzba and I. Zahed, Phys. Rev. **D62**, 034015 (2000) [hep-ph/9910347].
84. R. Rapp, E. Shuryak and I. Zahed, hep-ph/0008207.
85. D. T. Son and M. A. Stephanov, hep-ph/0005225.
86. For a review, see H. Heiselberg and M. Hjorth-Jensen, Phys. Rept. **328**, 237 (2000) [nucl-th/9902033].
87. N. K. Glendenning and F. Weber, astro-ph/0003426. See also D. Blaschke, H. Grigorian and G. Poghosyan, astro-ph/0008005.
88. M. van der Klis, to appear in Ann. Rev. Astronomy and Astrophysics, (2000) [astro-ph/0001167].
89. R. Wijnands and M. van der Klis, Nature **394**, 344 (1998); D. Chakrabarty and E. Morgan, Nature **394**, 346 (1998).
90. L. Bildsten, Astrophys. J. **501** L89 [astro-ph/9804325]; A. Andersson, D. I. Jones, K. D. Kokkotas and N. Stergioulas, astro-ph/0003426.
91. D. Blaschke, T. Klahn and D. N. Voskresensky, Astrophys. J. **533**, 406 (2000) [astro-ph/9908334]; D. Blaschke, H. Grigorian and D. N. Voskresensky, astro-ph/0009120.
92. D. Page, M. Prakash, J. M. Lattimer and A. Steiner, hep-ph/0005094.

93. C. Schaab *et al*, *Astrophys. J. Lett* **480** (1997) L111 and references therein.
94. T. Schäfer, hep-ph/0006034.
95. M. Alford, J. Bowers and K. Rajagopal, hep-ph/0008208.
96. G. W. Carter and S. Reddy, hep-ph/0005228.
97. J. Madsen, *Phys. Rev. Lett.* **85**, 10 (2000) [astro-ph/9912418] and references therein.
98. L. Bildsten and G. Ushomirsky, astro-ph/9911155.
99. D. Blaschke, D. M. Sedrakian and K. M. Shahabasian, *Astron. and Astrophys.* **350**, L47 (1999) [astro-ph/9904395].
100. M. Alford, J. Berges and K. Rajagopal, *Nucl. Phys.* **B571**, 269 (2000) [hep-ph/9910254].
101. For reviews, see J. Sauls, in *Timing Neutron Stars*, J. Ögleman and E. P. J. van den Heuvel, eds., (Kluwer, Dordrecht: 1989) 457; and D. Bhattacharya and G. Srinivasan, in *X-Ray Binaries*, W. H. G. Lewin, J. van Paradijs, and E. P. J. van den Heuvel eds., (Cambridge University Press, 1995) 495.
102. A. M. Clogston, *Phys. Rev. Lett.* **9**, 266 (1962); B. S. Chandrasekhar, *App. Phys. Lett.* **1**, 7 (1962).
103. P. F. Bedaque, hep-ph/9910247.
104. A. I. Larkin and Yu. N. Ovchinnikov, *Zh. Eksp. Teor. Fiz.* **47**, 1136 (1964); translation: *Sov. Phys. JETP* **20**, 762 (1965).
105. P. Fulde and R. A. Ferrell, *Phys. Rev.* **135**, A550 (1964).
106. M. A. Alpar and C. Ho, *Mon. Not. R. Astron. Soc.* **204**, 655 (1983). For a review, see A.G. Lyne in *Pulsars: Problems and Progress*, S. Johnston, M. A. Walker and M. Bailes, eds., 73 (ASP, 1996).
107. For reviews, see D. Pines and A. Alpar, *Nature* **316**, 27 (1985); D. Pines, in *Neutron Stars: Theory and Observation*, J. Ventura and D. Pines, eds., 57 (Kluwer, 1991); M. A. Alpar, in *The Lives of Neutron Stars*, M. A. Alpar et al., eds., 185 (Kluwer, 1995). For more recent developments and references to further work, see M. Ruderman, *Astrophys. J.* **382**, 587 (1991); R. I. Epstein and G. Baym, *Astrophys. J.* **387**, 276 (1992); M. A. Alpar, H. F. Chau, K. S. Cheng and D. Pines, *Astrophys. J.* **409**, 345 (1993); B. Link and R. I. Epstein, *Astrophys. J.* **457**, 844 (1996); M. Ruderman, T. Zhu, and K. Chen, *Astrophys. J.* **492**, 267 (1998); A. Sedrakian and J. M. Cordes, *Mon. Not. R. Astron. Soc.* **307**, 365 (1999).
108. R. Modler *et al.*, *Phys. Rev. Lett.* **76**, 1292 (1996).
109. P. W. Anderson and N. Itoh, *Nature* **256**, 25 (1975).
110. M. A. Alpar, *Astrophys. J.* **213**, 527 (1977).
111. M. A. Alpar, P. W. Anderson, D. Pines and J. Shaham, *Astrophys. J.* **278**, 791 (1984).
112. E. Witten, *Phys. Rev.* **D30**, 272 (1984).
113. E. Farhi and R. L. Jaffe, *Phys. Rev.* **D30**, 2379 (1984).
114. P. Haensel, J. L. Zdunik and R. Schaeffer, *Astron. Astrophys.* **160**, 121 (1986).
115. C. Alcock, E. Farhi and A. Olinto, *Phys. Rev. Lett.* **57**, 2088 (1986); *Astrophys. J.* **310**, 261 (1986).
116. N. K. Glendenning and F. Weber, *Astrophys. J.* **400**, 647 (1992).
117. A. Alpar, *Phys. Rev. Lett.* **58**, 2152 (1987).

- 118. J. Madsen, Phys. Rev. Lett. **61**, 2909 (1988).
- 119. R. R. Caldwell and J. L. Friedman, Phys. Lett. **B264**, 143 (1991).
- 120. X.-D. Li, I. Bombaci, M. Dey, J. Dey, E. P. J. van den Heuvel, Phys. Rev. Lett. **83**, 3776 (1999); X.-D. Li, S. Ray, J. Dey, M. Dey, I. Bombaci, Astrophys. J. **527**, L51 (1999); B. Datta, A. V. Thampan, I. Bombaci, astro-ph/9912173; I. Bombaci, astro-ph/0002524.
- 121. D. Psaltis and D. Chakrabarty, Astrophys. J. **521**, 332 (1999); D. Chakrabarty, Phys. World **13**, No. 2, 26 (2000).